

Supporting Information

Dual-targeted poly(amino acid) nanoparticles on-site deliver drug combinations: an intracellular synergistic strategy to eliminate intracellular bacteria

Dongdong Zhao^a, Wenli Feng^a, Xiaoxu Kang^a, Haofei Li^a, Fang Liu^b, Weitao Zheng^c, Guofeng Li^{a,*}, Xing Wang^{a,*}

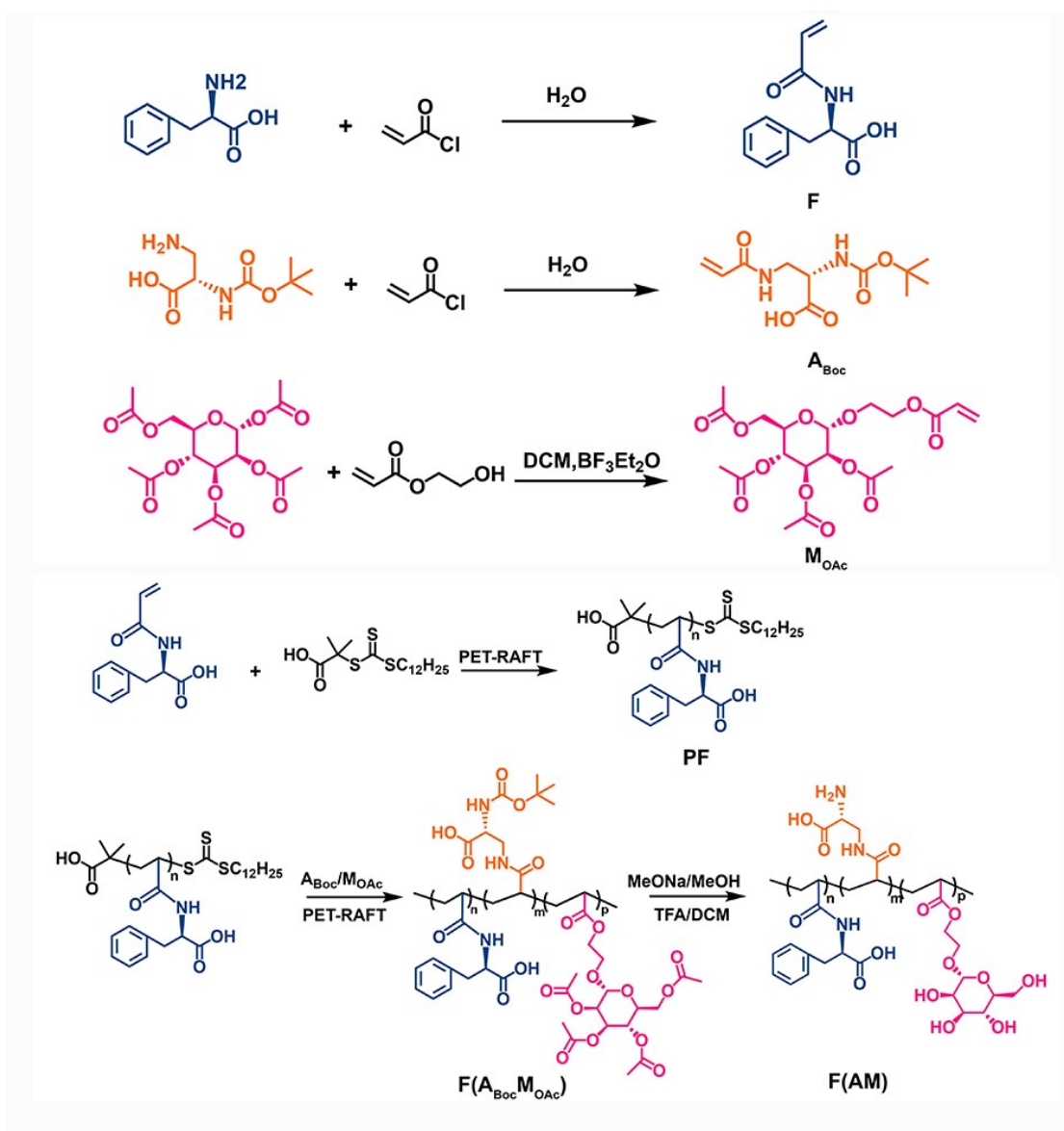
^a *State Key Laboratory of Organic-Inorganic Composites; Beijing Laboratory of Biomedical Materials, Beijing University of Chemical Technology, Beijing 100029, P. R. China*

^b *Department of Oncology of Integrative Chinese and Western Medicine, China-Japan Friendship Hospital, Beijing, 100029, China*

^c *Hubei Provincial Key Laboratory of Industrial Microbiology, Sino-German Biomedical Center, National “111” Center for Cellular Regulation and Molecular Pharmaceutics, Hubei University of Technology, Wuhan, 430068, Hubei Province, China*

* Corresponding author

E-mail address: ligf@mail.buct.edu.cn (G. Li); wangxing@mail.buct.edu.cn (X. Wang)



Scheme S1. Synthetic routes of the F, A_{Boc}, M_{OAc}, PF, and F(AM).

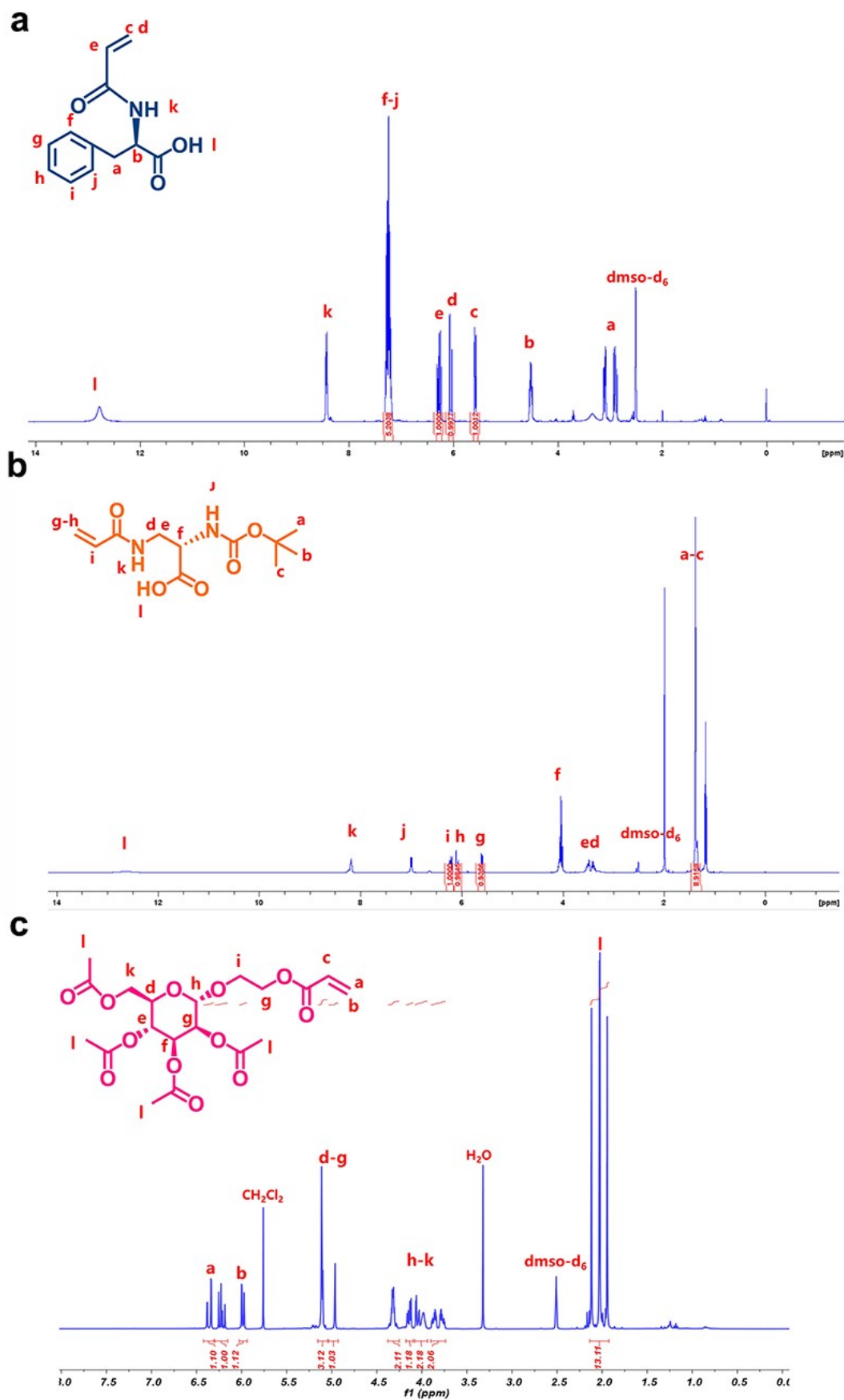


Figure S1. ^1H NMR spectra of (a) F, (b) A_{Boc} , and (c) M_{OAc} (400 MHz, $\text{DMSO-}d_6$).

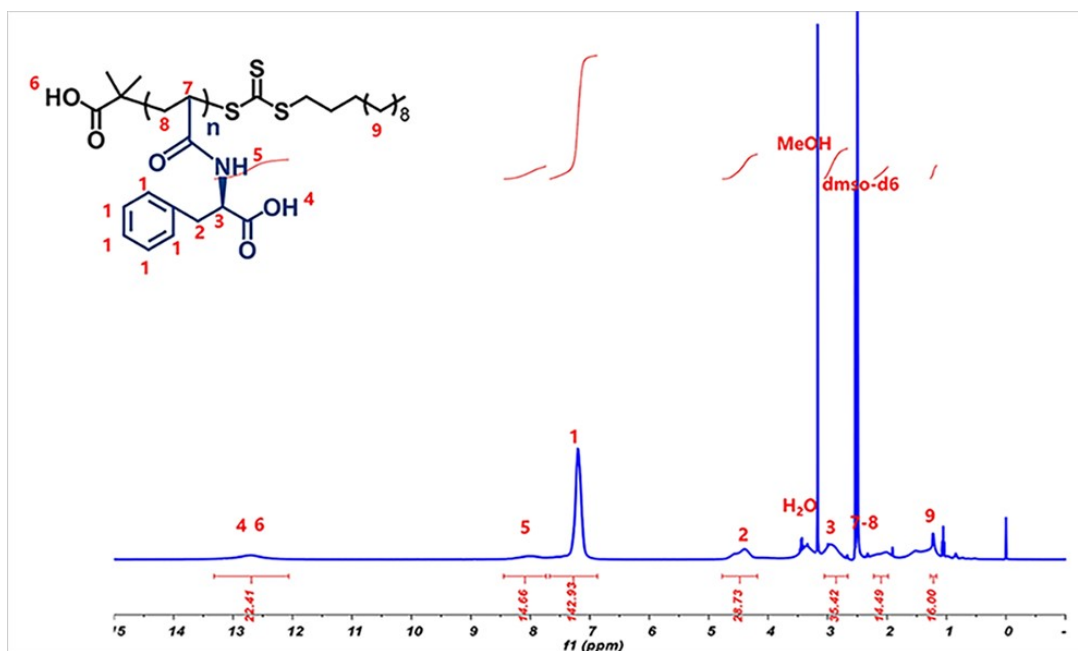


Figure S2. ^1H NMR spectrum of the PF (400 MHz, $\text{DMSO-}d_6$).

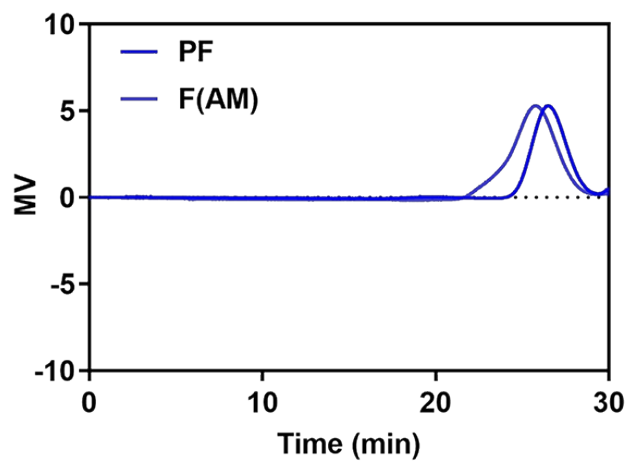


Figure S3. GPC curves of PF and F(AM).

Table S1. GPC analysis of PF and F(AM).

	Mn	PDI
PF	7069	1.34
F(AM)	11451	1.89

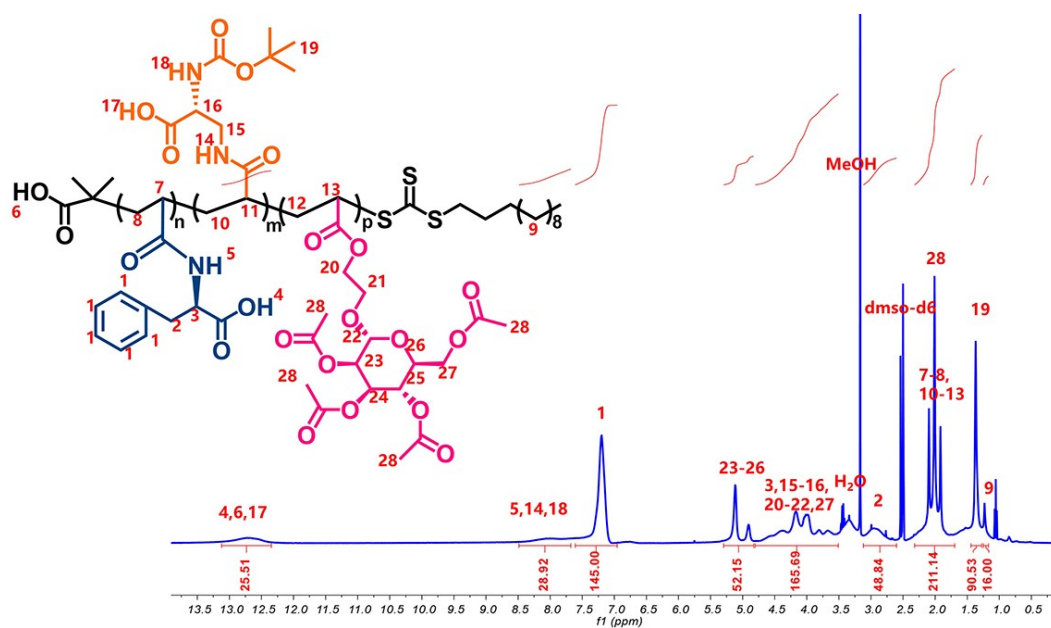


Figure S4. ^1H NMR spectrum of $\text{F}(\text{A}_{\text{Boc}}\text{M}_{\text{OAc}})$ (400 MHz, $\text{DMSO-}d_6$).

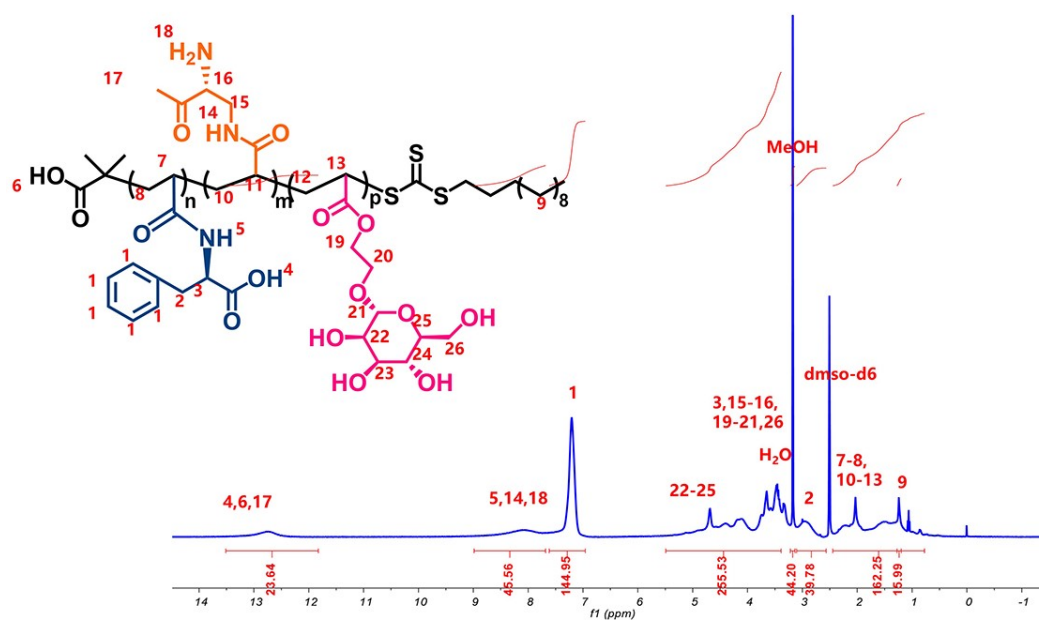


Figure S5. ^1H NMR spectrum of $\text{F}(\text{AM})$ (400 MHz, $\text{DMSO-}d_6$).

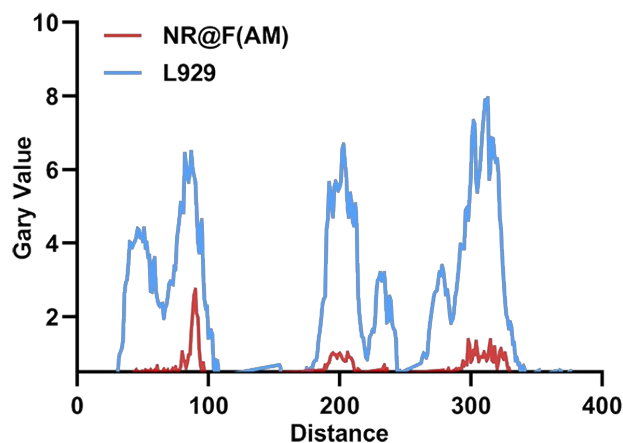


Figure S6. Co-localization fluorescence intensity distribution between NR@F(AM) NPs and L929 fibroblasts, which was analyzed using Image J software.

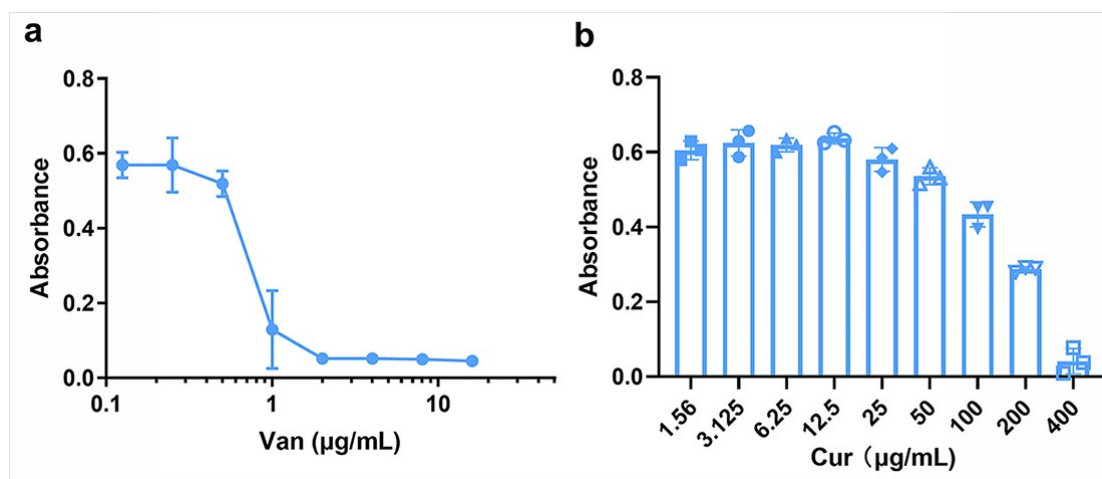


Figure S7. MIC assays of (a) Van and (b) Cur against MRSA.

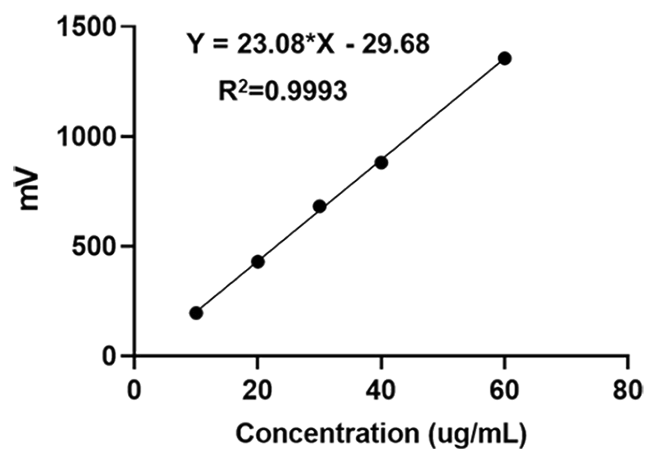


Figure S8. HPLC standard curve of Van. Van was monitored at a wavelength of 230 nm. The mobile phase composed of 0.01 mol/L potassium phosphate monobasic

monopotassium phosphate solution (pH 3.2) and methanol (spectroscopic grade) (80:20, v/v) at a flow rate of 1.0 mL/min.

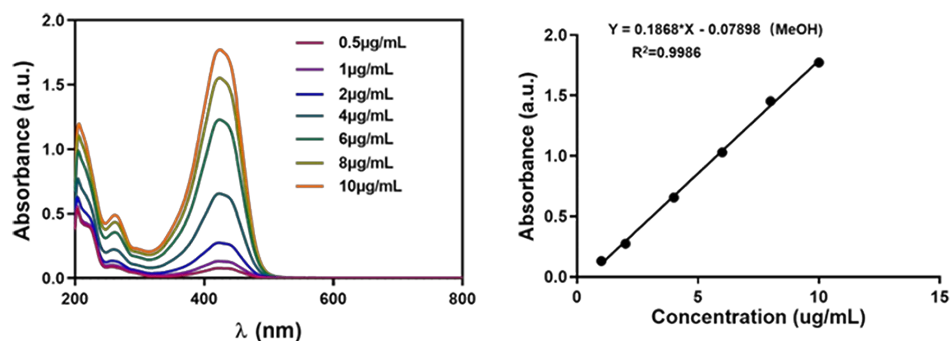


Figure S9. Absorption spectra of different concentrations of Cur in MeOH solution (left) and its standard curve at 425 nm wavelength (right).

Table S2. DLC and DLE of the (Van_{1.5}+CUR_{3.0})@F(AM) NPs.

	DLC(%)	DLE(%)
(Van _{1.5} +CUR _{3.0})@F(AM) NPs	(Van)13.5%	(Van)62.4%
	(Cur)23.2%	(Cur)54.9%

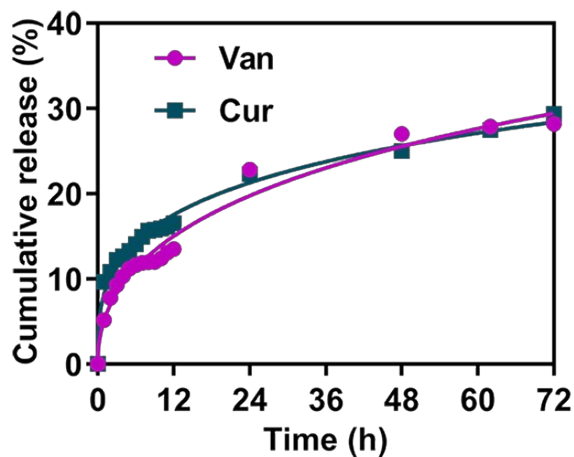


Figure S10. Release profiles of Van and Cur from (Van_{1.5}+Cur_{3.0})@F(AM) NPs.

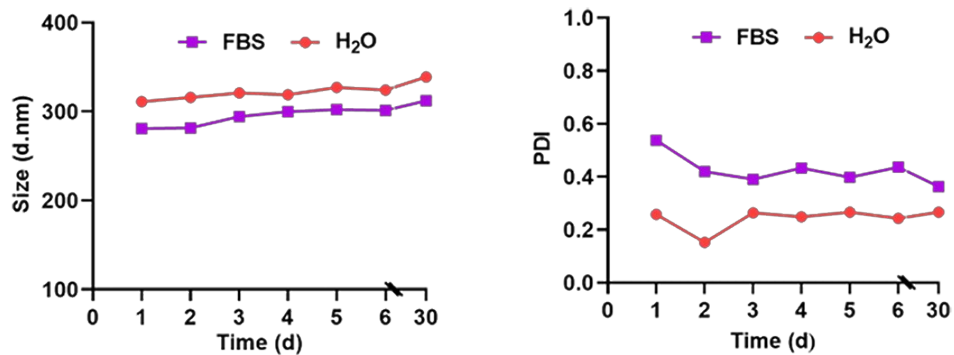


Figure S11. The variations of size and PDI of (Van_{1.5}+Cur_{3.0})@F(AM) NPs under different conditions (H₂O and 10% FBS).

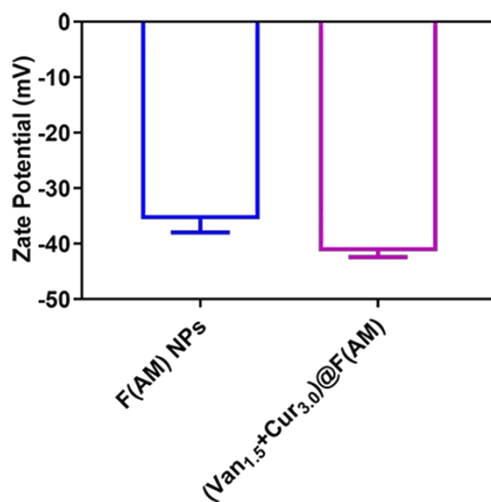


Figure S12. Zeta potential of F(AM) NPs and (Van_{1.5}+Cur_{3.0})@F(AM) NPs.

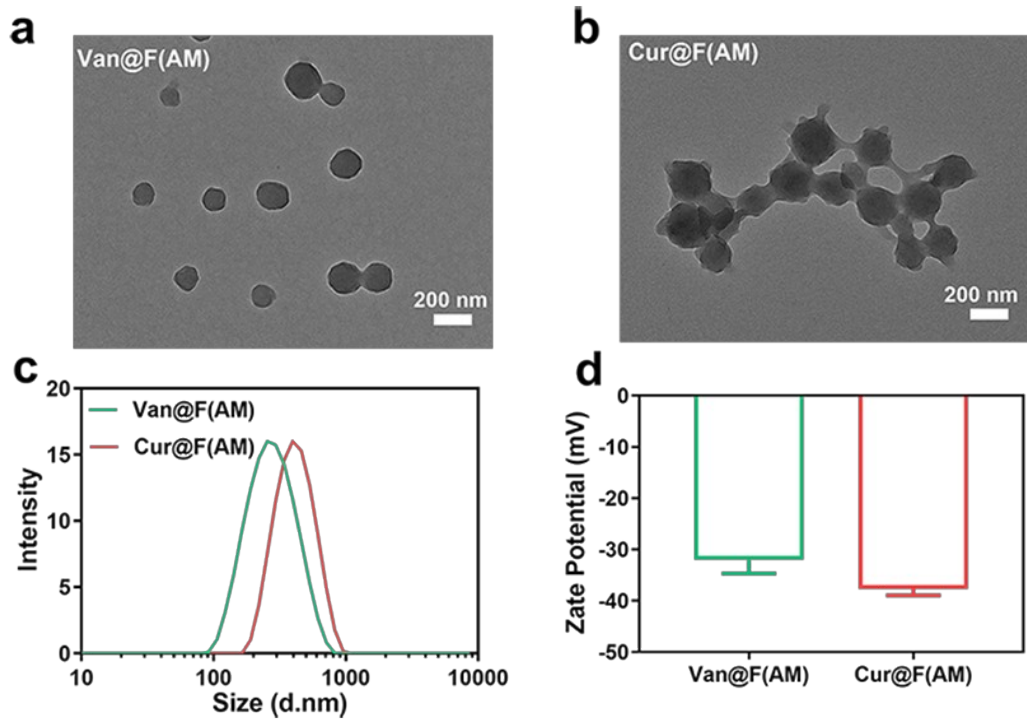


Figure S13. TEM image of (a) Van@F(AM) NPs and (b) Cur@F(AM) NPs. (c) Size distribution of Van@F(AM) NPs and Cur@F(AM) NPs, testing by DLS. (d) The zeta potential of Van@F(AM) NPs and Cur@F(AM) NPs.

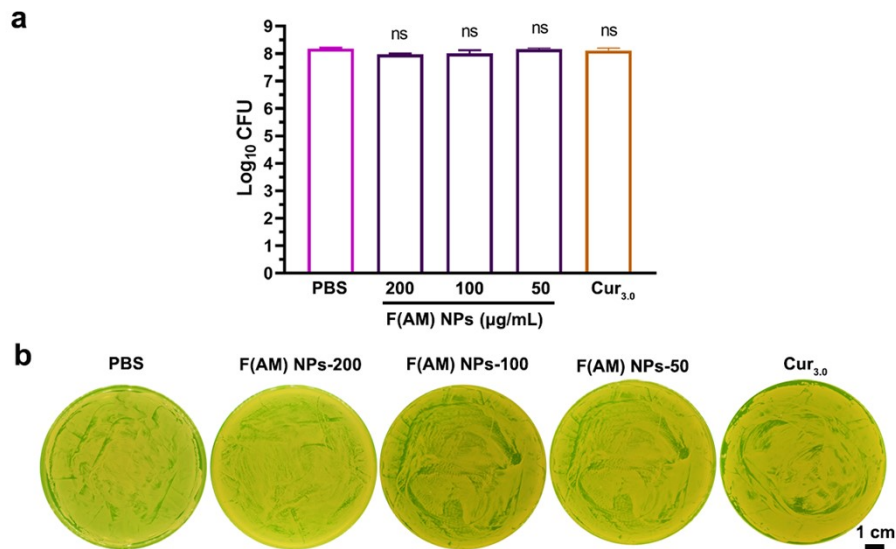


Figure S14. Intracellular antibacterial evaluation. (a) CFU count of intracellular MRSA after different treatments for 24 h. (b) CFU photographs of intracellular MRSA. ns $p > 0.05$, n = 3.

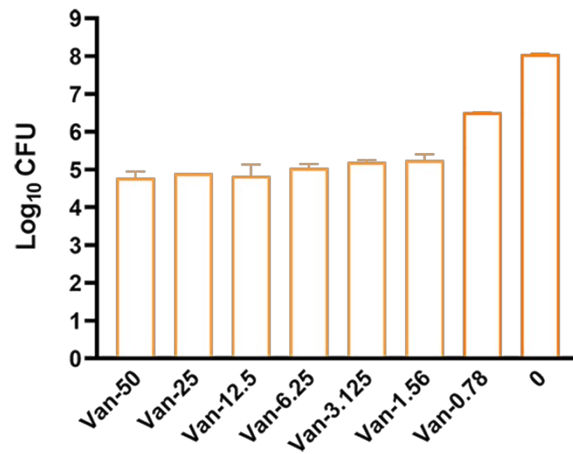


Figure S15. CFU of intracellular MRSA after treatment with different concentrations of Van ($\mu\text{g/mL}$).

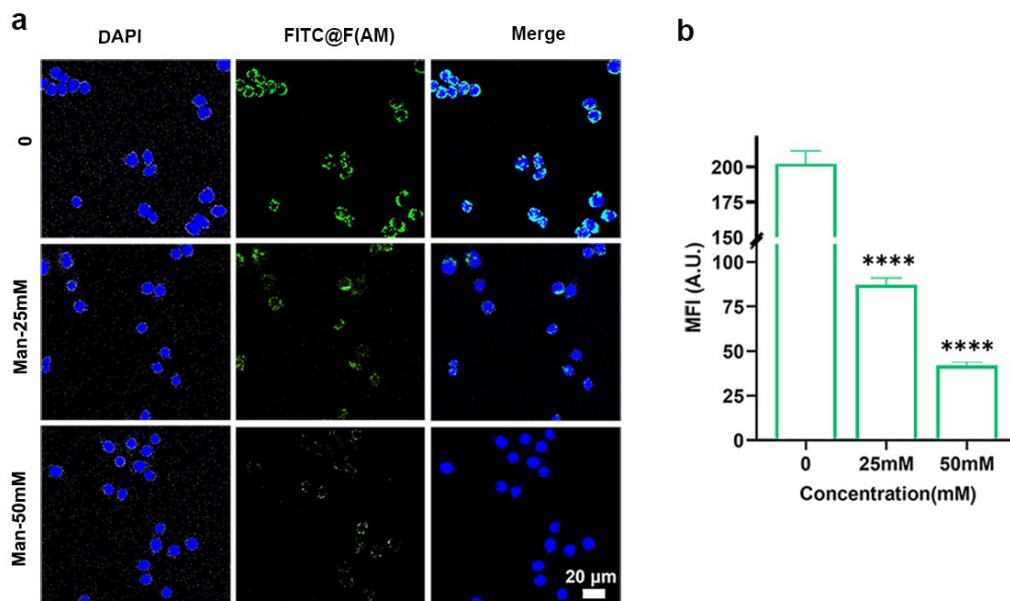


Figure S16. (a) CLSM observation of FITC@F(AM) NPs (green) in RAW264.7 macrophages and (b) analysis of fluorescence intensity using Image J software. (**** $p < 0.0001$, $n = 6$).

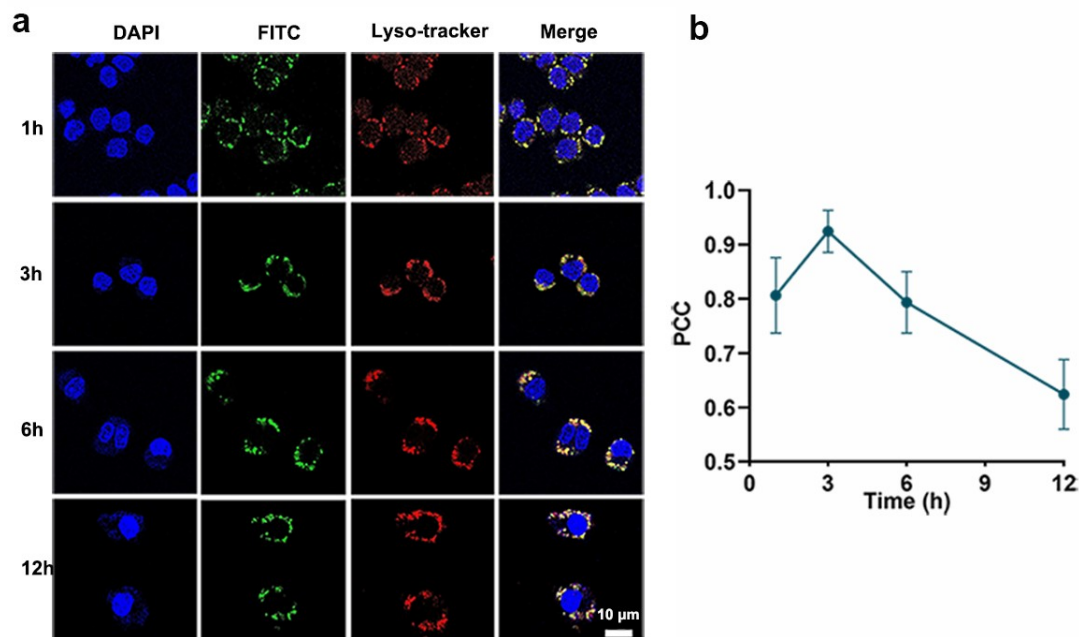


Figure S17. (a) CLSM observation of co-localization between FITC-labeled NPs (green) and LysoTracker (red) in RAW264.7 macrophages. (b) Evolution with the time of the Pearson's correlation coefficients between the signals from the FITC-labeled NPs and LysoTracker.

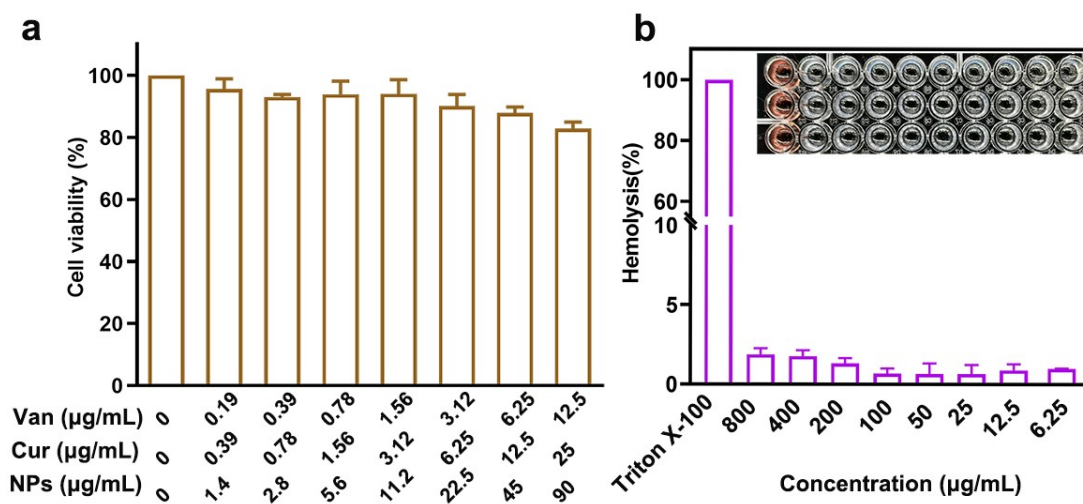


Figure S18. (a) The cell cytotoxicity of (Van+Cur)@F(AM) NPs against RAW264.7 macrophage. (b) The hemolysis rate of (Van+Cur)@F(AM) NPs with different concentrations.

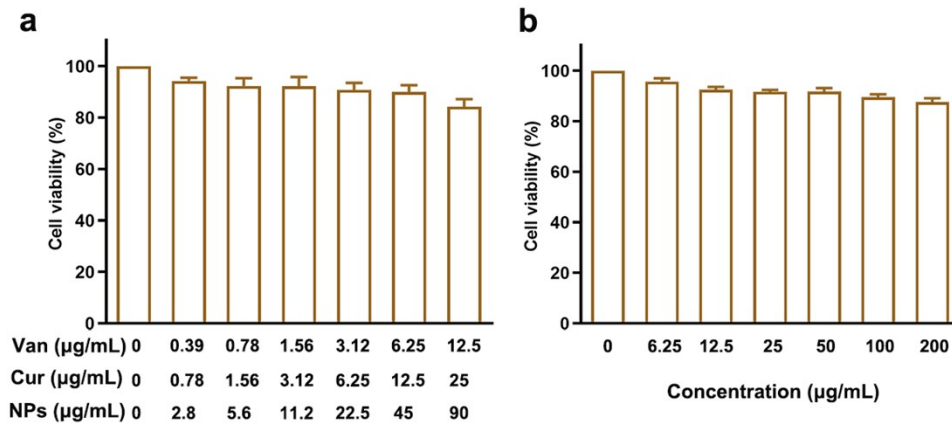


Figure S19. (a) The cell cytotoxicity of (Van+Cur)@F(AM) NPs against L929 fibroblasts. (b) The cell cytotoxicity of F(AM) NPs against L929 fibroblasts.

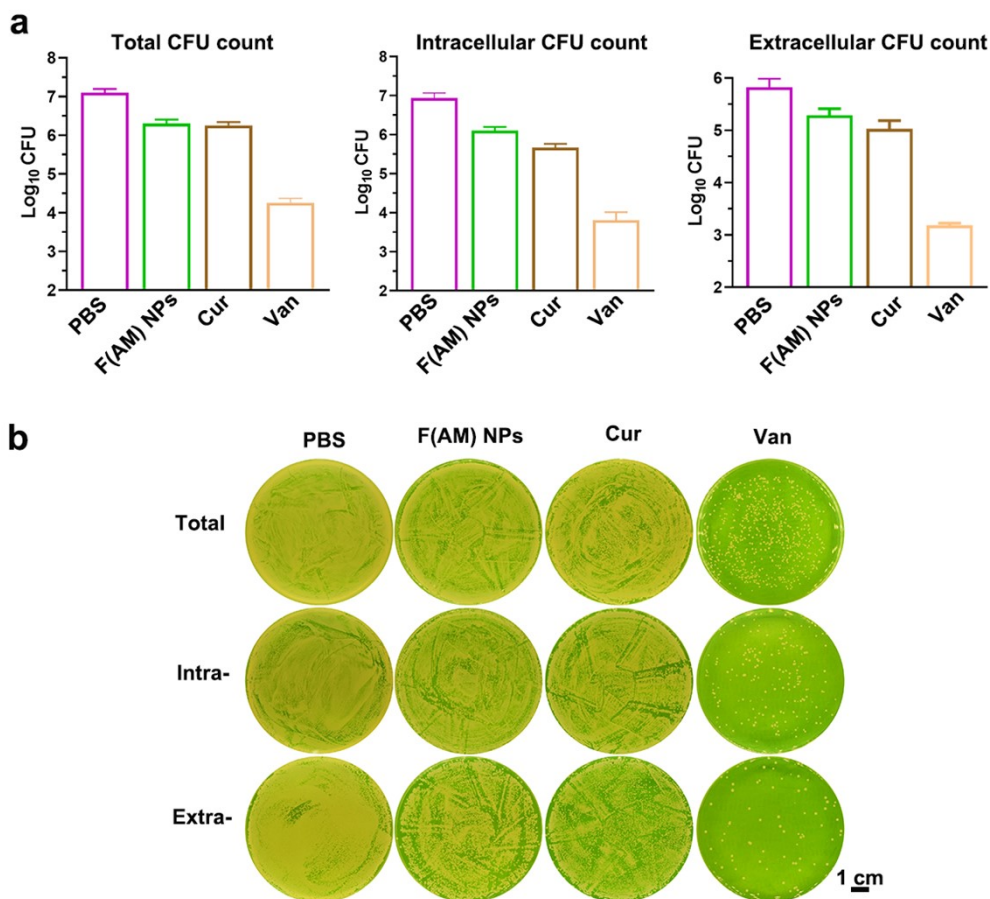


Figure S20. The in vivo antibacterial assays of Van (10 mg/kg), Cur (20 mg/kg) and F(AM) NPs (20 mg/kg). (a) CFUs in total, intracellular and extracellular fractions. (b) CFU photographs.

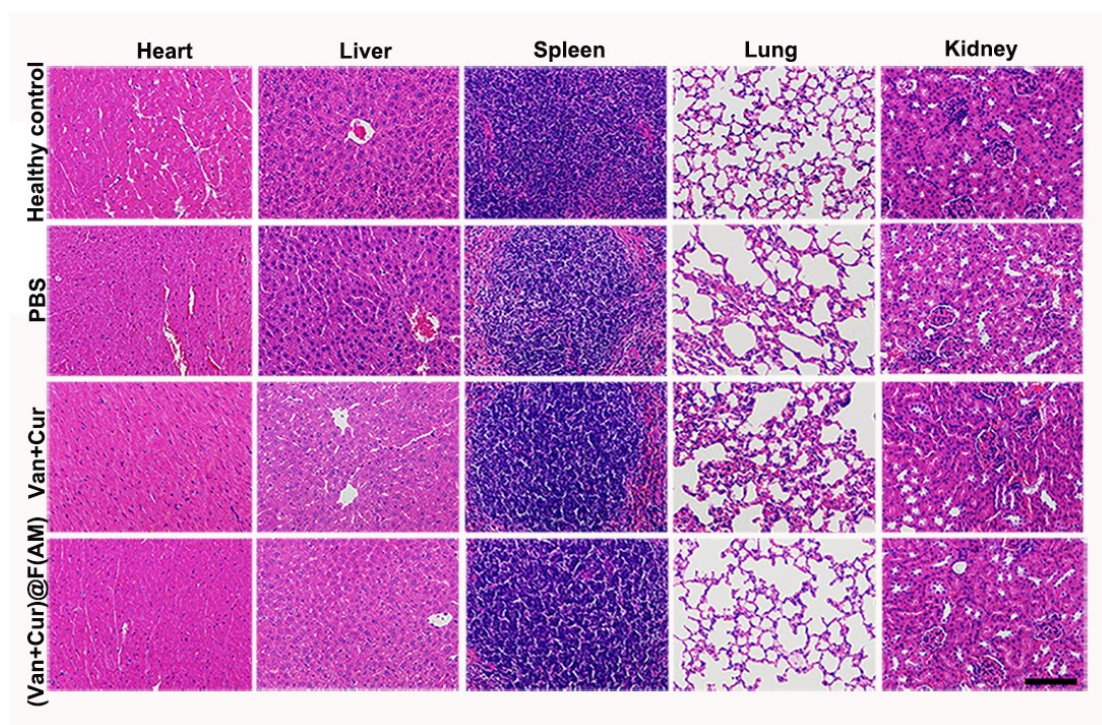


Figure S21. Representative H&E staining images of various organs from mice treated with healthy control, PBS, Van+Cur, and (Van+Cur)@F(AM) NPs (10 mg/kg Van, 20 mg/kg Cur). Scale bars: 200 μ m.